Application of Computational Kinetic Mechanism Generation to Model the Autocatalytic Pyrolysis of Methane

ARTICLE *in* INDUSTRIAL & ENGINEERING CHEMISTRY RESEARCH · MARCH 2003

Impact Factor: 2.59 · DOI: 10.1021/ie020581w

4 AUTHORS, INCLUDING:

Ioannis Androulakis
Rutgers, The State University of New Jersey
198 PUBLICATIONS **2,846** CITATIONS
SEE PROFILE

Anthony M Dean
Colorado School of Mines
158 PUBLICATIONS **3,933** CITATIONS
SEE PROFILE

Application of Computational Kinetic Mechanism Generation to Model the Autocatalytic Pyrolysis of Methane

Jeffrey M. Grenda,* Ioannis P. Androulakis, and Anthony M. Dean†

Corporate Strategic Research, ExxonMobil Research & Engineering Company, Annandale, New Jersey 08801

William H. Green, Jr.

Department of Chemical Engineering, Massachusetts Institute of Technology, Cambridge, Massachusetts 02139

An automated computational mechanism-generation technique is applied to construct elementary-step chemical kinetic reaction models for the pyrolysis of methane at 1038 K and 0.58 atm. Under these conditions, the pyrolysis process is extremely complex and exhibits autocatalysis. The mechanism-generation approach constructs a detailed set of elementary reactions, retrieves or estimates required reaction rates and thermochemistry, and constructs a kinetic model that gives excellent agreement with experimental data for several species. Key to the success is a newly developed capability of the algorithm to identify pressure-dependent chemically activated reactions. A rate-based species-selection methodology is used to determine kinetically significant species, and the algorithm is demonstrated to identify critical low-concentration byproducts. Multistep chemically activated reactions involving the formation of cyclopentadiene and subsequent hydrogen atom production are found to be important reactions, agreeing with previous literature findings. The present work demonstrates that computer-generated kinetic models can quantitatively predict experimental behavior for conditions where reaction rate constants and thermochemistry are reasonably well established. Several topics are also presented that outline areas of ongoing research.

Introduction

For about two decades, it has been recognized that the process of constructing chemical kinetic models could be computationally automated and that this would be extremely helpful in predicting or simulating the complex free-radical chemistry of pyrolysis and combustion. This ongoing research has been primarily motivated by the fact that manually constructed mechanisms are extremely time- and labor-intensive to develop even for simple model fuels. This is not surprising given the large number of species and reactions that can occur, the requirement of accurate estimations of thermodynamic properties and reaction rates, and the need to determine which species and reaction pathways are significant.

Several groups have developed kinetic-model-generation approaches[1−10] and used them for a variety of homogeneous gas-phase chemistry applications. Similar work has also been used extensively and successfully to model catalytic processes[11] for complex feeds typical of petroleum applications. Given the tremendous number of potentially important species and kinetic reactions for representative fuel feeds, the increasing use of computer-generated kinetic models will likely be required if we are ever to model the elementary chemical reaction details of processes involving important complex materials such as gasoline and jet fuel.

A major conceptual and algorithmic challenge in applying computational kinetic modeling techniques is determining which chemical species and reactions should be included in the kinetic model. Clearly, this challenge is analogous to the difficulties faced by the kineticist pursuing manual mechanism model development. It is highly desirable to keep the model as small as possible to speed computations and improve understanding. However, it is far from clear how the computer should determine whether particular species or reactions belong in the mechanism. Our rate-based selection algorithm[12] appears to be a viable proposal for handling this difficult problem. In the current work, we present an application to methane pyrolysis, a difficult system with extremely nonlinear multistep autocatalysis[13] that provides a severe test of the robustness of the rate-based algorithm.

Typical existing kinetic-model-construction algorithms are based on a series of rules that describe known elementary reaction steps, and structural algorithms that identify and manage reactant and product species. Given a generated reaction, the parameters required to compute the reaction rate $k(T)$ as a function of temperature are needed. These are often expressed in a modified Arrhenius form on the basis of experimental data, quantum chemical calculations, or Evans−Polanyi correlations.

For combustion chemistry applications, chemically activated reactions often play a significant role in the system reaction kinetics. Such reactions involve highly energized nonthermalized species that undergo rapid internal isomerization or dissociation before collisional stabilization. The energized nonthermal intermediates are sufficiently short-lived that these reactions appear to be direct elementary reactions between the thermalized species, but the chemical changes between reac-

* Corresponding author. Tel.: (908)730-2545. Fax: (908)-730-3344. E-mail: jeffrey.m.grenda@exxonmobil.com.

† Present address: Department of Chemical Engineering, Colorado School of Mines, Golden, CO 80401.

10.1021/ie020581w CCC: $25.00
Published on Web 01/28/2003

tants and products reflect the multistep nature of the process. The typical approach of building the mechanism computationally considers only classical single-step high-pressure-limit elementary reactions and fails to identify these important pathways, potentially leading to significant errors. Because each of the energized intermediate adducts involves a coupled system of competing multistep isomerization and deactivation pathways, the overall rate constants for the apparent reactions exhibit complex pressure and temperature dependencies. If the pressure dependence due to falloff or chemical activation is known for a particular reaction, $k(T,P)$ can be given in one of several complicated forms. For a computer algorithm to construct accurate kinetic models, these chemically activated processes should be included in the construction process. The availability of accurate rate constant libraries and methods for estimating unknown rate constants is critical and remains the primary challenge in employing automated mechanism-generation techniques. The current focus is on demonstrating that one can construct pressure-dependent reaction pathways using mechanism generation to capture the kinetics of autocatalytic systems.

To facilitate comparison with previous literature and manually developed mechanisms, we have deliberately used equivalent thermodynamic parameters of existing analyses.[13] The methane pyrolysis problem serves as a good validation example case that, although apparently simple, exhibits highly nonlinear and surprisingly complex kinetics. Recent modeling[14] has modified the reported thermochemical properties of cyclopentadienyl, which impacts the accepted understanding of pyrolysis kinetics and reaction pathways. Using improved values for the thermodynamic parameters and some of the rate coefficients, important new reaction channels in methane pyrolysis have been identified.[15] In the current work, we demonstrate an example for methane pyrolysis where the omission of chemically activated pathways leads to substantial disagreement with experimental data. The results described should be viewed as a validation of the approach used to construct mechanisms rather than an attempt to validate a particular mechanism. The current work is the first demonstration of an automated mechanism approach constructing chemically activated reaction pathways in the course of the mechanism-generation process.

Computational Mechanism-Generation Algorithm

The computational approach is a structure-based method that represents molecular structures and chemical reactions using planar graphs and matrix manipulation algorithms.[9,16,17] The industrial version of the code known as XMG (ExxonMobil mechanism-generation code)[18,19] is used in the model development research. This approach is based on previous work of Klein and Broadbelt,[9,10] and many of the core species identification and manipulation routines are taken from this previous work. The current version includes newly developed algorithms for the construction of pressure-dependent chemically activated reaction pathways, detailed thermodynamic reversibility and reaction rate consistency, automatic character-based nomenclature, structural string generation, and coupling with group additivity thermochemistry estimation,[20] as well as coupling with advanced mechanism reduction techniques.[21] Although not the focus here, the code can also be used in stand-alone mode to explore and compute $k(T,P)$ for individually specified pressure-dependent reaction channels.[22,23] The purpose of the current work is to incorporate the pressure-dependent channel algorithm into the overall mechanism-generation algorithm and to demonstrate the importance of including chemical activation channels in the predictive capability of the algorithm.

Mathematical Representation of Species and Chemically Activated Reactions. Existing kinetic-model-construction algorithms fail to accurately model pressure-dependent chemically activated reactions. The primary reason for this deficiency is that most chemically activated reactions consist of a series of elementary steps that form a coupled system. The methyl radical recombination reaction plays an important role in the methane pyrolysis system and is an example of a chemically activated approach where the initial reactants form a unimolecular product with a single exit channel. Matrix species representations and the method of computing chemical reactions for this case are shown in Figure 1. Further details can be found in the literature[9,10] for high-pressure reactions. The following discussion emphasizes the unique ability of the current approach to consider chemically activated reactions. The bond and electron (BE) matrix[16] representation for methyl radical is shown in the upper left-hand side matrix in Figure 1. The atoms are arbitrarily numbered, and each atom corresponds to a row and column of a connectivity matrix. Atom connectivity is given by nonzero entries equal to the bond order in the off-diagonal locations of the matrix. Radicals include an entry on the diagonal of the matrix element containing the unpaired electron. The numbering for methyl radical is shown above the matrix in the top left of Figure 1. Different initial atom numberings result in different matrices but identical bonding. The algorithms used to determine unique string nomenclatures for each species are built on canonical structures, and details can be found in the literature.[9,16,17]

Chemical reactions are performed by permuting entries in the reactant matrix bonding. A list of possible reaction families is maintained, and proposed reactants are tested systematically to determine whether the required atomic reactive sites exist for the given reaction family. The key to the approach is the fact that chemical reactions typically involve only a small number of reactive atomic sites relative to the total number of atoms in the reactants. A reaction matrix can be represented compactly for large arbitrarily bonded species and is a key advantage in performing computational reactions.

Returning to the chemically activated methyl radical recombination reaction shown in Figure 1, in the upper left corner, the two methyl radical matrices are combined to form a single reactant matrix. Inspection of this matrix indicates that the entries are such that the two original distinct species are retained, with different atom numbering. A query of the possible reaction families indicates that radical recombination is a plausible reaction for the initial reactant matrix. To perform a chemical reaction, the participating atom sites are collected in the upper left-hand corner of the matrix. Matrix manipulation routines taken from Klein and Broadbelt[9,10] are used to perform the required row and column permutations. Each reaction family can be assigned a concise matrix that will perform the required connectivity changes to model the reaction. The reaction

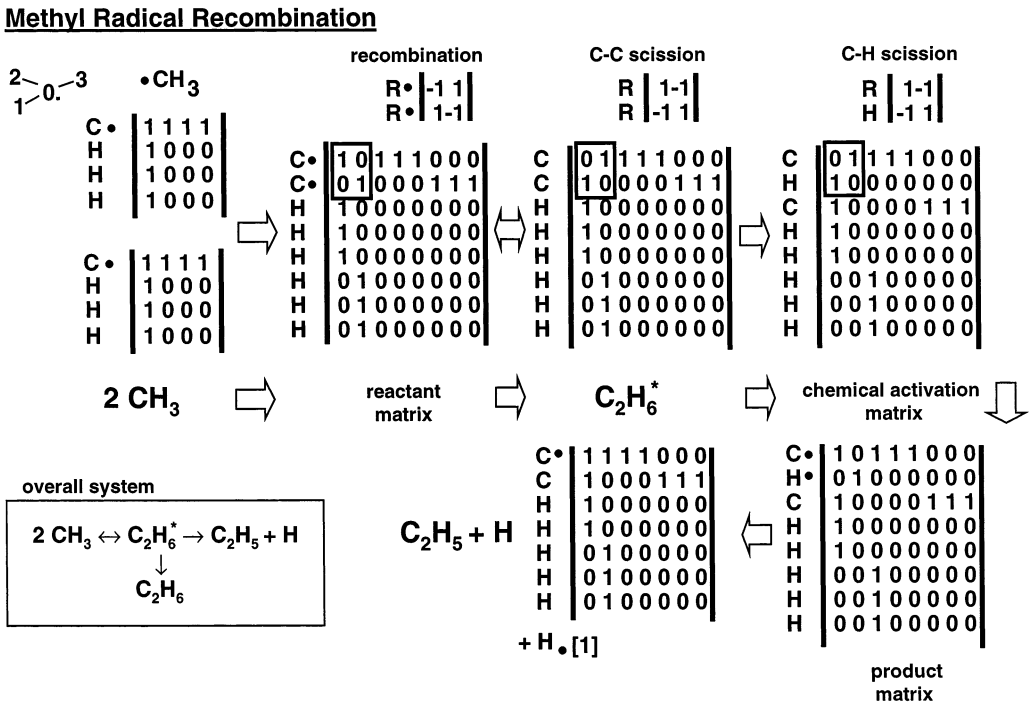

Figure 1. Matrix operations for the chemically activated recombination of methyl radical. A temporary reactant matrix is formed, and several reaction matrices are applied to the unimolecular energized adduct. The product species are deconvolved from the final product matrix to form the system of reactions. For this simple system, the energized adduct can either return to reactants, further react to produce ethyl radical + H, or be collisionally stabilized. The overall reaction pathway structure is shown in the inset at left.

matrix for radical recombination is noted above the reactant matrix in Figure 1.

To perform the reaction, the reaction matrix is added to the upper left corner of the reactant matrix (effectively a padded matrix addition), and the resulting matrix shown to the right indicates that the energized ethane adduct C_2H_6* has been formed from the recombination. The species structure is noted by the algorithm as energetically excited, and the algorithm proceeds to explore for possible further isomerization or decomposition reactions. The possible reaction pathways are first determined with no consideration of reaction rate values. A search of the possible reaction families indicates that this species can undergo scission of either the carbon−carbon bond, or one of the six identical carbon−hydrogen bonds. The reaction matrix for C−C bond scission is shown above the adduct matrix in Figure 1, and application of the matrix will result in a reverse reaction to the original reactant matrices. The chemical activation matrix is reorganized to collect a representative C−H site in the upper left corner of the matrix to perform the C−H bond scission. This is shown in the top right matrix of Figure 1. Application of the reaction matrix forms the product matrix shown in the bottom right of Figure 1, and the algorithm deconvolves the product matrix into the product matrices ethyl radical + H. The final reaction pathway for the energized adduct is that of collisional stabilization, which is an identity matrix transformation to a stabilized product, or $C_2H_6^* \rightarrow C_2H_6$. The overall set of chemically activated reaction pathways is summarized in the bottom left of Figure 1. The set of overall apparent reactions involving the thermalized species are then predicted to be $CH_3 + CH_3 = C_2H_6$, $CH_3 + CH_3 = H + C_2H_5$, and $C_2H_6 = H + C_2H_5$. In the current approach, reaction rate constants for the overall reactions in the system are determined from a database of QRRK,[25] RRKM, or experimental reaction rate constants as functions of pressure and temperature.

The previous example illustrates the systematic search method used to identify all chemically activated reaction pathways. The algorithm maintains a connected tree structure of chemically activated adducts, and the tree structure is developed on-line as the reaction mechanism is constructed. When a unimolecular product is formed from an entrance reaction, a series of proposed subsequent unimolecular reactions is queried and considered. If determined to be possible, the reactions are executed, analyzed, and stored in the developing tree structure. If further unimolecular isomerization is realized, then a new excited adduct is formed and is recursively handled as an entry in the chemically activated reaction system. A set of bimolecular products, such as from a β-scission reaction, form an exit channel and are not considered further. The assumption is that much of the chemical energy released in exothermic reactions forming multiple products goes into the external rotational modes and the relative translation of the products, so that the product species are not themselves chemically activated. Once the entire system has been explored and all possible energized adducts have been formed, a complete set of overall apparent reaction channels can be written.

An example considering a more complex multistep chemical activation reaction is the radical addition reaction of allyl to acetylene, which is illustrated in Figure 2. As before, the initial reactant species are combined to form a reactant matrix. The reaction matrix contains three reactive atom sites: the radical site of the attacking radical and the unsaturated carbon−carbon bond. The addition reaction matrix is shown above the reactant matrix and is applied to form a carbon−carbon bond between the radical site and one of the unsaturated acetylene carbons, reducing the order

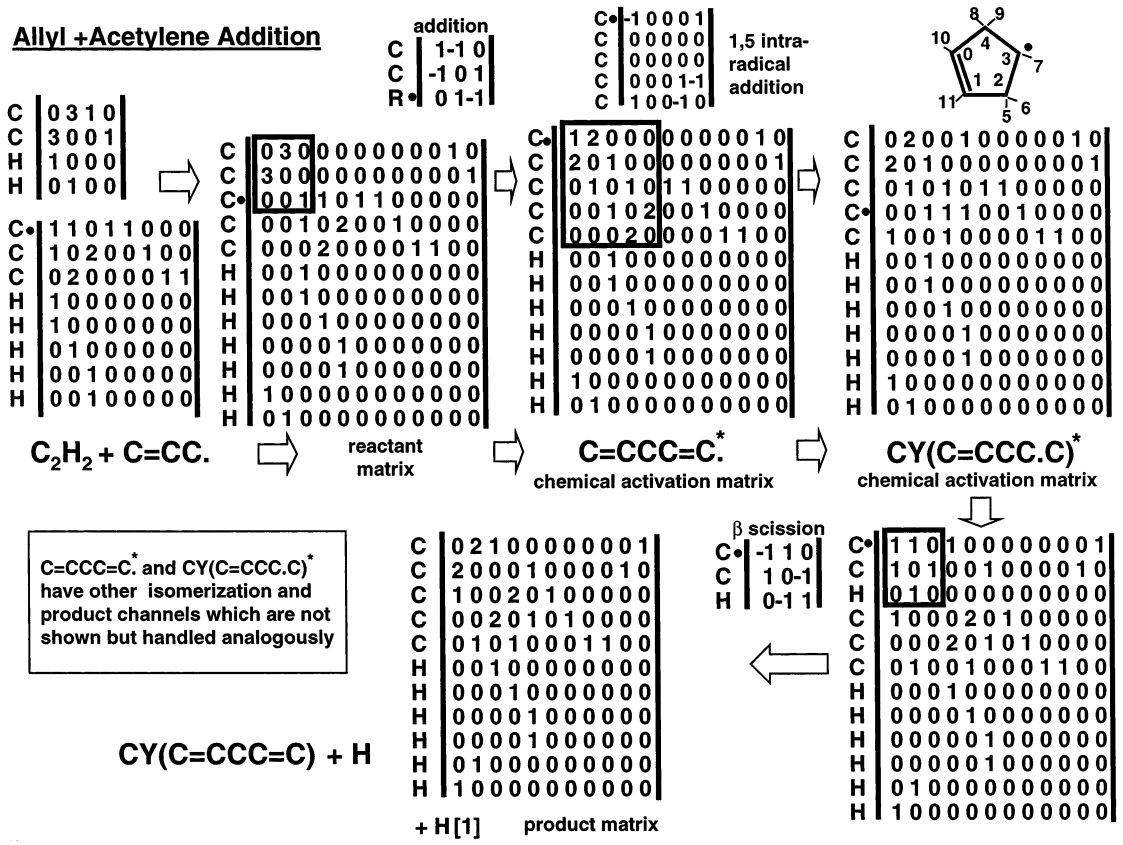

Figure 2. Matrix operations for the chemically activated radical addition of allyl to acetylene. The multistep chemically activated pathway sequence of allyl + acetylene producing cyclopentadiene + H is shown. Numerous additional channels resulting from isomerization of the intermediate energized adducts are not shown for brevity. The developing chemically activated pathway structures are used to generate overall apparent reactions that are included in the mechanism-generation procedure.

of the bond and appropriately moving the radical site. The product matrix to the right of the reactant matrix in Figure 2 now contains the representation for the energized product 1,4-pentadien-1-yl radical (the notation C═CCC═C*· is used where ═ represents a double bond and · denotes the radical site). Under lower-temperature and higher-pressure conditions, the collisional stabilization of the initially formed adduct is likely dominant, and the overall reaction would be C_2H_2 + C═CC· = C═CCC═C·. This is the method used in conventional mechanism-generation approaches. At lower pressures and higher temperatures, however, isomerization of the adduct can lead to a series of additional reaction pathways before the radical is thermalized by collisions with the bath gas. As before, the current algorithm treats the formed adduct C═CCC═C*· as energetically excited and then explores for further isomerization or decomposition reactions.

A search of the reaction templates indicates that the activated adduct can be collisionally quenched; decompose to the initial reactants; isomerize through hydrogen shifting; or form cyclic intermediates through intraradical addition, where the radical site can add to either unsaturated carbon atom. Addition to the primary carbon involves five atoms, the radical site and attached carbon backbone terminating with an unsaturated bond, as seen in the 1,5 intraradical addition matrix shown at the top of Figure 2. Application of this reaction matrix to the chemically activated matrix produces the energized cyclopenten-4-yl radical CY(C═CCC·C)*, shown in the top right of Figure 2. This species is similarly noted as an energized adduct, and the algorithm again recursively explores for possible further isomerization or decomposition reactions. This search reveals a viable β-scission pathway, and the matrix is reorganized in the lower right of Figure 2 to apply the given β-scission reaction operator to the C−H site. The resulting product matrix is shown to produce the bimolecular channel cyclopentadiene CY(C═CCC═C) + H.

Numerous other coupled channels are computed and included but not shown in Figure 2 for simplicity. Hydrogen shift reactions from the C═CCC═C*· adduct produce C═CC·C═C* and C═CCC·═C* as possible intermediates, with vinyl radical C═C· and propadiene (allene) C═C═C as examples of possible products. Similarly, intraradical addition to the secondary unsaturated carbon forms cyclobutenylcarbinyl radical C·CY(CC═CC)*, a much less thermodynamically favorable pathway relative to that shown in Figure 2. All of the excited intermediate adducts can also be collisionally stabilized and are included and stored in the coupled system. It is important to note that the algorithm captures all of the possible pathways and maintains them in a connected tree structure for the estimation of the reaction rate constants of the overall apparent reactions.

Having identified the chemically activated reaction channels for this system, we query available reaction databases for reaction rate constant estimates of $k(T,P)$, as many of the kinetically important reactions for methane pyrolysis have previously been compiled. In the present work, we discard chemically activated reactions whose reaction rate constants are unavailable in the database. This implies that the pathways were judged insignificant in the off-line manual QRRK analyses used to compile the database. This approach can

Table 1. Example Thermodynamic Predictions Obtained from the Group Additivity Estimation Procedure Coupled Directly to the Mechanism-Generation Algorithm[a]

species	Hf[b]	Sf[b]	Cp300	400	500	600	800	1000	1500		
CCC	−25.33	64.50	17.88	22.63	27.05	30.93	37.11	41.88	49.36	C3	H8
CCC·	23.67	69.29	17.11	21.27	25.14	28.53	33.95	38.14	44.70	C3	H7
CC·C	21.02	70.31	16.38	20.30	23.95	27.54	33.36	37.43	44.16	C3	H7
CCCC	−30.26	73.92	23.38	29.58	35.30	40.28	48.18	54.22	63.56	C4	H10
CC(C)C	−32.50	70.43	23.11	29.52	35.37	40.42	48.37	54.36	63.92	C4	H10
C*CCC	−0.11	73.61	20.57	26.09	31.04	35.28	41.96	46.97	54.75	C4	H8
CC*CC	−3.22	72.39	20.70	25.74	30.42	34.58	41.34	46.44	54.40	C4	H8
C*CC·C	33.39	69.80	19.03	24.27	28.96	32.96	39.21	43.83	50.90	C4	H7
C*CCC·	48.89	78.40	19.80	24.73	29.13	32.88	38.80	43.23	50.09	C4	H7
C*CC(C)C	−6.53	80.34	25.80	32.98	39.46	44.77	53.22	59.45	69.25	C5	H10
C*CC·(C)C	24.77	76.65	24.01	30.60	36.72	41.80	49.94	55.90	65.18	C5	H9
CY(CCCCC)	−18.74	70.00	19.93	28.24	35.86	42.32	52.29	59.48	70.25	C5	H10
CY(C*CCCC)	7.82	70.62	19.56	26.79	33.22	38.57	46.73	52.57	61.31	C5	H8
CY(C*CC*CC)	31.26	66.87	18.14	24.69	30.22	34.66	41.21	45.78	52.56	C5	H6

[a] Data used to compute NASA coefficients for determining required temperature-dependent thermodynamic properties. Group contribution values are taken from the NJIT Database[24] of Bozzelli et al. [b] Units: enthalpy, kcal/mol; entropy, cal/mol/K; specific heat, cal/mol/K.

work effectively when the database contains accurate estimates of the important reactions, but it relies on the accuracy of the database systems to ensure that missing channels are unimportant.

It would certainly be better if the $k(T,P)$ values could be estimated during the mechanism-construction procedure. Our ongoing research is focused on directly coupling a $k(T,P)$ estimation procedure into the model-construction algorithm[15] and will allow us to test the reliability of the current procedure. For larger chemically activated adducts, an enormous number of isomerizations are possible, making it impractical to directly and accurately compute all of the $k(T,P)$ reaction rates. To enable this, we have constructed a numerical screening procedure to avoid including isomers and reactions that are negligible under the conditions of interest[22] and a criterion for determining whether $k(T,P)$ will differ significantly from $k_\infty(T)$ for a reaction through a large adduct without requiring the full $k(T,P)$ calculation. These techniques will serve as effective screening methods to enable the computation of large chemically activated systems.

Estimation of Thermochemistry. Accurate estimations of the enthalpy and entropy are critical in obtaining accurate reaction rates estimates, obtain proper energy balances, and ensuring reaction microscopic reversibility. From a computational perspective, this accuracy is especially important because it eliminates the need for reaction rate estimate rules in both reaction directions, thus simplifying the approach. For reactions written identically in both directions (such as abstractions), a preferred reaction direction is specified on the basis of exothermicity.

The computational mechanism-generation procedure provides challenges in that the number of species considered can be large and the structure of the product species cannot be determined ahead of time and might be complex. A fast and reasonably accurate estimation procedure is required for those species that cannot be located in appropriate literature database libraries. This is accomplished through coupling with an automated group additivity approach to estimate thermochemical and physical properties of molecules and radicals.[20,24] The approach utilizes a large existing database of group contributions[24] required for the accurate estimation of radicals critical to combustion chemistry applications. Representative examples of the thermodynamic data utilized by the mechanism-generation procedure are shown in Table 1. The additivity approach makes estimates of the heat and entropy of formation and the heat capacity at several discrete temperatures for use with reaction rate constant estimation rules described below. The calculation of reduced frequencies for use with QRRK[25] analyses is also automatically performed.

Estimation of Reaction Rates $k_\infty(T)$. The kinetic-model-construction process depends on the ability to identify kinetically significant reactions for the conditions of interest and to estimate their high-pressure-limit rate constants $k_\infty(T)$. Reaction-identification and rate-estimation rules of different levels of complexity have been included for a wide variety of reaction families important in hydrocarbon pyrolysis and oxidation systems. Important reaction families include inter- and intramolecular abstraction, intramolecular addition, recombination/dissociation, and addition/β-scission. Rate estimates for several dozen of these reaction families have been detailed in recent publications.[26−32]

Newly developed rate-estimation rules that are used in the current approach incorporate substantial material from the literature and include a significant amount of structural detail in assembling the hierarchy of rules for reactant rate constant estimation. This information includes examples such as the bond type and location within the species, the effect of resonant stabilization and bond strength, the number and effect of rotor losses on reaction intermediates, and ring-strain in the transition state. The rate constant rules include special estimation rules for reactions involving unique radical species such as H, O, OH, CH_3, etc. Reactions that have been studied with great detail and have experimental or ab initio modeling estimates available can be retrieved from a reaction rate constant archive.

Automatic Generation of Species Nomenclature. As shown earlier in Figures 1 and 2, the molecular structure is represented as a connected graph and decomposed iteratively into unique substituents that can be reconstructed systematically to generate a unique lexigraphical and parenthetical string nomenclature used to identify species uniquely.[9] Simple examples of unique molecular strings include $C(H_3)C(H_3)$ for ethane, $C[C(H_2)C(H_3)H]$ for propene, and $C(H)C(H)C(H)C(H)C(H_2)$ for 1,3-cyclopentadiene. Although such strings serve the critical purpose of identifying species uniquely, this nomenclature is extremely burdensome for the kinetic modeler to interpret manually. To address this problem, we have developed an automated species

```
CH4 => CH3 + H                    C2H5 + C2H5 => CCCC
CH3 + H => CH4                    CCCC => C2H5 + C2H5
CH4 +H => CH3 + H2                CCCC => CCC.C + H
CH3 + H2 => CH4 + H               CCCC => CCCC. + H
CH3 + CH3 => C2H6                 C=CC + C2H3 => C=CC. + C2H4
CH3 + CH3 => C2H5 + H             C=CC + CH4 => CCC. + CH3
C2H6 => CH3 + CH3                 C=CC + CH4 => CC.C + CH3
C2H6 => C2H5 + H                  C2H4 + C=CC => C2H5 + C.=CC
C2H5 + H => C2H6                  C2H4 + C=CC => C2H5 + C=C.C
C2H6 + H => C2H5 + H2             C2H4 + C=CC => C2H5 + C=CC.
C2H5 + H => CH3 + CH3             CCC.C => C=CC + CH3
C=CC + CH3 => C.=CC + CH4         CCC.C => C=CCC + H
C=CC + CH3 => C=C.C + CH4         CCC.C + CH3 => C=CCC + CH4
C=CC + CH3 => C=CC. + CH4         CCC.C + H => C=CCC + H2
```

Figure 3. Representative output of generated elementary reactions and overall apparent chemically activated reactions from the automated chemical reaction generation algorithm. Internal matrix representations of species are translated into readable string nomenclature. Simple common species names such as methane or hydrogen are taken from a database. Other more complex species are named using a newly developed species-nomenclature-generation algorithm.

nomenclature generator based on the convention of Bozzelli[24] that parses arbitrary species into readable strings. Our computer-generated nomenclature gives CC, CC═C, and CY(C═CC═CC) for ethane, propene, and cyclopentadiene, respectively. We maintain a check that prevents two isomers from being assigned the same user-readable name. Common species names are used if defined in a database, such as the nomenclature C_2H_6 and C_2H_5 for ethane and ethyl radical, respectively. A short list of representative reactions is given in Figure 3, illustrating the format of the elementary reactions generated and output of the approach, and highlights the relative ease by which the reactions can be interpreted for use with manual mechanism-construction efforts. It is our experience that the capability to construct and output a detailed, human-readable mechanism transparent to differences between manual and automated construction is a key modeling capability and can be used as a powerful modeling tool.

Species Selection and Model Construction. A challenging aspect of kinetic model construction is devising species-selection and model-generation algorithms that capture important species and reactions but that avoid including unnecessary species or reactions. In the current work, the model is constructed iteratively, using a modified version of the rate-based algorithm.[12] Kinetically significant species (called "reacted") appear as reactants and products in the model, and "unreacted" species appear only as products. To construct the mechanism, the algorithm selects the species from the unreacted species pool that has the largest kinetic production rate. The algorithm then generates all possible reactions of the species with itself and with previous reacted species, increasing the reaction model size and adding any new unknown species to the unreacted species pool. For each single-product reaction, the algorithm is extended as described previously to treat that reaction as chemically activated, and so it undergoes an arbitrary series of unimolecular isomerization reactions, terminated either by collisional quenching or by the production of exit products. Once all reactions are found, the original reactant species is then redesignated a reacted species. The new larger reaction scheme is solved, and the resulting temporal species concentrations are used to repeat the entire process until all of the remaining unreacted species are formed at rates below user-specified tolerances. One defined model-construction procedure convergence criterion can be written as[12]

$$R_j(t) < \epsilon R_{\text{char}}(t) \qquad \forall j \in \{\text{reacted species}\} \qquad t_o < t < t_o + \tau \quad (1)$$

where R_j is the formation rate of the jth unreacted species computed using the current kinetic model, τ is the user-specified time scale of the simulation, ϵ is the user-specified tolerance, and the symbols indicate that species j is included from the reacted species set. In the present work, we defined the characteristic rate R_{char} as the formation rate of the species with the maximum current rate of production.

Note that, as the algorithm progresses and reacts available species together to generate chemical reactions, species whose production rates are initially determined to be unimportant are continually being reevaluated to assess whether they have evolved to be significant. The rate-based algorithm has the important advantage of converging to a model that includes kinetically significant species but relatively few unimportant species. In contrast, most model-construction algorithms presented in the literature do not include any rate-based significance test and might miss important species and reactions and include unimportant pathways. However, tight tolerances might be required to ensure that all of the minor species important in a stiff nonlinear autocatalytic system are included. This is particularly true for cases where the autocatalysis loop involves several elementary steps, because the kinetic importance of this loop will not become evident until several of the species involved have been identified as significant.

The methane pyrolysis case has such character and provides an excellent test of the robustness of the species-selection criterion used by the algorithm, as well as of the importance of including the chemically activated channels. The kinetics of this system are also extremely nonlinear during the induction phase, provid-

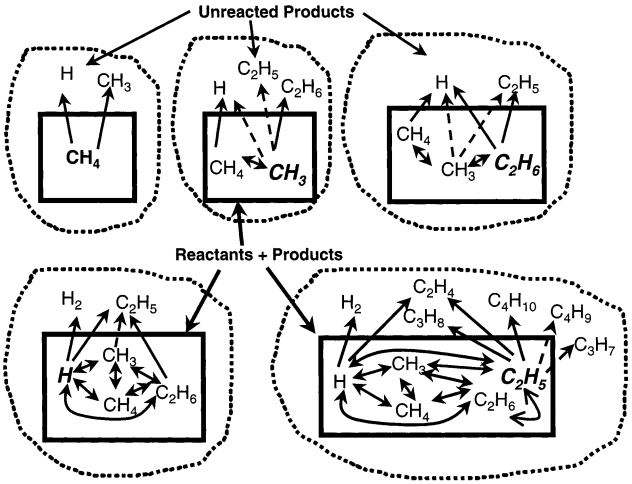

Figure 4. Iterative construction of the kinetic mechanism for the pyrolysis of methane. Species that appear as both reactants and products (reacted) are enclosed by solid box. Edge (unreacted) product species are continually evaluated for inclusion as reactants in the developing model. Dashed lines indicate multistep chemically activated reactions that would be missed by conventional model-construction algorithms. Some arrows have been omitted for clarity.

ing a particularly stringent test of the rate-based species-selection criterion. To illustrate the effects of changing the tolerance ϵ and the importance of identifying the chemically activated channels, a variety of simulations are presented in the following section.

Model Predictions and Comparison with Experimental Data. The process for mechanism construction of methane pyrolysis is illustrated in Figure 4. In the first step in the top right of Figure 4, the original neat methane has undergone C−H initiation reactions to produce methyl radicals and H atoms. At this point, the species lists include CH_4 as a reacted species and H and CH_3 as unreacted species. After two quick iterations, H and CH_3 have been included in the model, generating the new product species ethane, H_2, and ethyl radical (C_2H_5). The lines leading to C_2H_5 and H are drawn differently to indicate that this product set is only formed by a multistep chemically activated reaction; conventional high-pressure-limit-based model-generation programs would omit this step. After two more iterations, ethane and H have been included as reactive species, significantly improving the model. However, in the following iteration, the ethyl radical is incorporated into the model, and this opens up many channels leading to new species, including several additional chemically activated channels. The growth to higher-molecular-weight species begins through recombination reactions to form propane and butane and chemically activated routes to propyl radical and butyl radical. At this point, a major product, ethene, is first identified. It is clear that the numbers of generated species and reactions grow rapidly. The mechanism-generation process is iterated several dozen more times before the completeness criterion of eq 1 is satisfied to our specified precision.

The predictions of these computer-generated models are compared with the experimental data in Figures 5−7. The operating conditions of $T = 1058$ K and $P = 0.58$ atm were selected to be consistent with available experimental data.[33,34] The solid lines show the numerical predictions for different product species as a function of time, and the symbols represent available experimental data.

Figure 5 shows a comparison between numerical predictions and experimental measurements for the production of ethane versus time. The significant induction period, after which the production of ethane begins to accelerate nonlinearly, can be readily seen in the experimental data. Several numerical predictions are shown in Figure 5. The second curve from the bottom labeled "no chemical activation" considers only reactions written in the high-pressure limit and ignores channels that are chemically activated. In this case, which is characteristic of existing computational mechanism-generation approaches, the induction time is not captured. The ethane production growth occurs very slowly and does not reach the levels of the experiment even over a long time period. Several additional curves are shown in Figure 5 that include the new capability of incorporating chemically activated reactions. A discussion of the restricted reactions (dashed) curve is postponed temporarily. The remaining numerical predictions (solid lines) in Figure 5 vary the level of precision selected as defined by eq 1. For the precision level of $\epsilon = 0.1$ (larger precision level magnitudes are equivalent to less strict tolerances in eq 1), the temporal predictions of the ethane levels still remain in disagreement with the experimental values, as, within this tolerance level, the growth of the mechanism to include higher-molecular-weight species has not occurred. Only a small number of species (17) have been included in the mechanism at this termination criterion. Numerical tests have shown that, for a variety of systems, precision levels usually less than 1% of the maximum species production rate are required to adequately capture the underlying detail of the radical chemistry. When the tolerance used is $\epsilon = 0.01$, the agreement between the predicted and experimental values improves significantly. The acceleration of ethane is captured, as higher-molecular-weight species have begun to be included in the mechanism. As the tolerance is tightened further by an order of magnitude, some additional improvement is seen in the agreement. Further restriction of precision results in effectively nonobservable macroscopic changes in the results. Clearly, the agreement of the model predictions with experiment requires the incorporation of chemically activated channels in the mechanism-construction procedure.

The ethylene yields obtained from each of the model predictions are compared with experiment in Figure 6. In the shorter time frame, the agreement between all models is close, but neither the low-precision nor high-pressure-limit approaches are able to capture the gradual increase in production at later times, consistent with the underprediction of the acceleration of ethane shown earlier in Figure 5. Some additional improvements are again seen in the agreement between the model and experiment with tightening levels of precision ranging from $\epsilon = 0.1$ to $\epsilon = 0.001$. The predicted propylene yields are presented in Figure 7 and show gradually improving agreement to the experimental data over ranges of precision varying over 3 orders of magnitude from $\epsilon = 0.1$ to $\epsilon = 0.001$. No significant adjustment of rate constants from our existing database was performed in an effort to improve the fit of the data. It is also possible that disagreements with experiment might also be attributed to missing chemical activation pathways

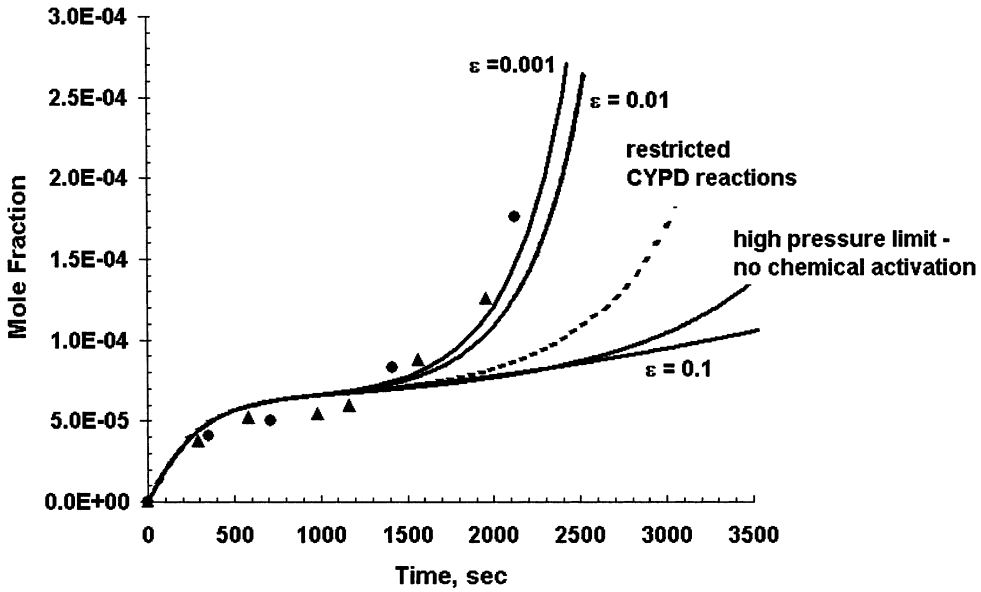

Figure 5. Model predictions vs experimental data (refs 33 and 34) for the production of ethane from methane pyrolysis at $T = 1038$ K and $P = 0.58$ atm. Good agreement of the model predictions (lines) with the experimental data (symbols) is obtained when multistep chemically activated reactions are included (using parameters from ref 13) and tight tolerances are employed during model construction. The accuracy improves as the precision parameter ϵ (eq 1) decreases from 0.1 to 0.001. The restricted CYPD reactions calculation omits chemically activated pathways leading to cyclopentadiene. The high-pressure-limit calculation omits all chemically activated reactions.

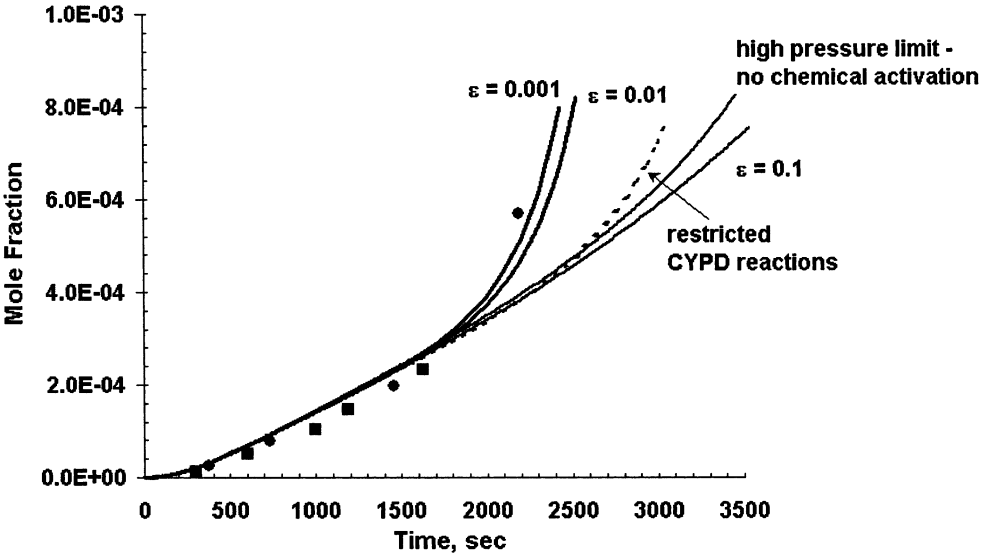

Figure 6. Model predictions vs experimental data (refs 33 and 34) for the production of ethylene from methane pyrolysis at $T = 1038$ K and $P = 0.58$ atm. Symbols are experimental data, lines are model predictions at precision levels (eq 1) ranging from $\epsilon = 0.1$ to $\epsilon = 0.001$. Good agreement is observed when chemically activated reactions are included in the model construction with increasing precision ranging from $\epsilon = 0.1$ to 0.001. The restricted CYPD reactions calculation omits chemically activated pathways leading to cyclopentadiene. The high-pressure-limit calculation considers reactions only in traditional high-pressure limit.

within the database. This is currently an area of continued research.

In Figures 5−7, several reaction channels appear responsible for the difference in the predictions between the chemically activated and high-pressure-limit mechanism-construction cases. The first, noted earlier, is the direct production of ethyl radical and hydrogen atom from methyl recombination, with the overall reaction written as $CH_3 + CH_3 = C_2H_5 + H$. This accelerates the overall conversion of methane by providing a radical chain-propagation step that competes with the chain-terminating recombination to form ethane. A second important chemically activated reaction is that illustrated earlier for the addition of allyl to acetylene, whose products include the unimolecular channels C═CCC═C·, C═CC·C═C, C═CCC·═C, CY(C═CCC·C), and C·CY(CC═CC), plus the bimolecular channels CY(C═CC═CC) + H and C═C· + C═C═C·. The algorithm is capable of identifying the important chemically activated reaction pathways such as these by constructing them from a combination of several elementary steps. The $k(T,P)$ values are then obtained from available database values.

The decomposition of cyclopentadiene eventually becomes an important source of radicals in this system, consistent with previous findings.[13] This was verified through both flux and sensitivity analyses. The important chemically activated reaction pathways found computationally are those for the direct production of cyclized radical species from activated linear adducts.

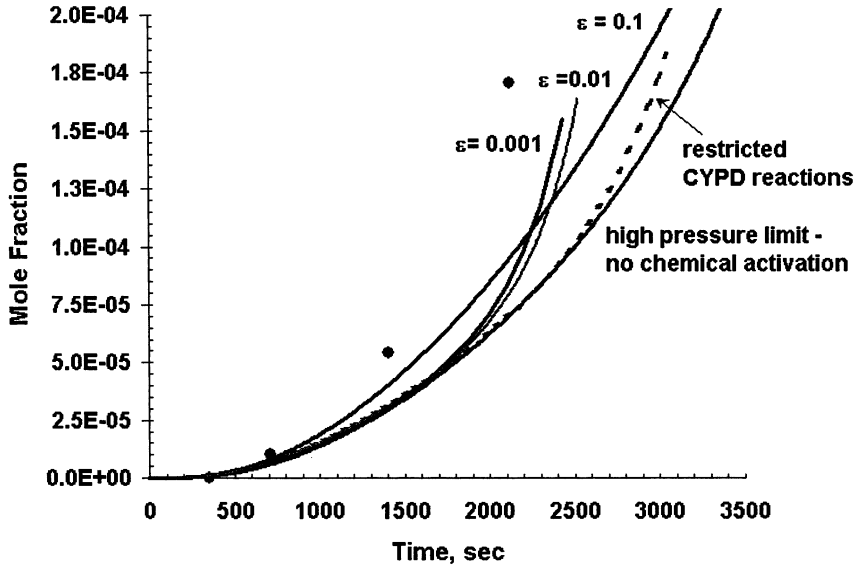

Figure 7. Model predictions vs experimental data (refs 33 and 34) for the production of propylene from methane pyrolysis at $T = 1038$ K and $P = 0.58$ atm. Symbols are experimental data, lines are numerical predictions that show fair agreement with data with increasing precision levels ($\epsilon = 0.1-0.001$). The high-pressure-limit calculation does not include chemically activated reactions, and the restricted CYPD reactions calculation omits chemically activated pathways leading to cyclopentadiene (both $\epsilon = 0.001$).

Several reactions provide various routes leading to cyclopentadiene, which subsequently forms cyclopentadienyl radical by either unimolecular dissociation or hydrogen abstraction. These reactions serve effectively as chain-branching steps that result in rapidly increased ethane production after a significant induction time for the accumulation of required species. To show the importance of this process, the numerical algorithm was modified to disregard chemically activated pathways leading to cyclopentadiene and instead to consider the entrance reaction to the chemically activated system to be in the high-pressure limit. The numerical results are given by the dashed curves labeled "restricted CYPD reactions" in Figures 5−7. In Figure 5, the acceleration of the ethane production occurs substantially more slowly, intermediate between the high-precision chemical activation results and the high-pressure-limit case. The differences in the results with the high-pressure-limit case illustrate the contribution of other chemically activated reactions to the process, and the differences with the high-precision numerical calculations illustrate the importance of the cyclopentadiene production and subsequent cyclopentadienyl pathways. Similar results can be noted for the restricted channel results (dashed lines) in Figures 6 and 7, where the omitted pathway reactions result in substantial disagreement with the experimental data.

The current problem is a decidedly nonlinear process, as some of the key species are initially insignificant, but the rate-based algorithm correctly identifies these species as becoming important several minutes into the pyrolysis when a sufficiently tight tolerance is used. This indicates the algorithm is capable of identifying as significant minor species that undergo a complex series of reactions only by considering the instantaneous species production rates. This approach appears to work even if the overall system kinetics are significantly nonlinear and have a broad range of important time scales.

The excellent agreement between the computer-generated model and the experimental data suggests that the model-construction algorithm has captured most important reaction paths. The rate-based species-selection procedure appears to be quite robust, correctly capturing low-concentration kinetically significant species and identifying chemically activated reaction paths that lead to autocatalysis. The computations reported here are good tests of the ability of our mechanism-generation algorithm to correctly identify the important species and reaction pathways, assuming that one can compute the corresponding rates and molecular properties. Methane pyrolysis is a favorable case, where many of the required rate constant estimates already exist and can be recalled from rate parameter databases. For this case, however, the algorithm identified many chemically activated reaction channels that were assumed negligible and discarded them because no chemically activated reaction rate constants were available from the QRRK database analyses. Current research underway is developing automated routines for accurately computing any unknown chemically activated rates [$k(T,P)$] during the mechanism-construction process to fill in the gaps in the reaction libraries.[15] Similar problems arise with respect to thermochemical and physical parameters and high-pressure-limit rate constants $k_\infty(T)$. It is clear that improved and expanded reaction rate constant estimation rules will be required before accurate detailed models of the chemistry of practical fuels become practical.

Conclusions

The current work has illustrated the application of automated computational mechanism generation to develop models to predict the products of methane pyrolysis at moderate temperature and pressure. The computer-generated kinetic model, which reflects the highly nonlinear kinetics of this autocatalytic process, is shown to agree well with available experimental data for several product species. Key to the success of the approach is the newly developed capability of the mechanism-generation algorithm to consider pressure-dependent chemically activated reactions. The rate-based species-selection methodology used to determine kinetically significant species is here demonstrated to

recognize low concentration but kinetically significant species under extremely nonlinear temporal production conditions.

The new algorithm provides increased confidence that the predictions are not in error because particular species or reactions were arbitrarily left out. The algorithm is capable of identifying significant species by considering the instantaneous species production rate as a function of time even if its concentration is small and the overall kinetics are significantly nonlinear. The algorithm monitors species that are numerically significant and solves the system of differential equations to a user-specified level of precision. Essentially, the user need only input the initial concentrations, the desired degree of conversion and precision, and a set of estimation rules, and the computer will generate the set of significant reactions, intermediates, and products and their concentrations as a function of time.

A critical aspect of the calculations is the accuracy to which species thermochemistry and reaction rate constant values can be assigned. Many of these values are unknown or have significant uncertainty, and these are undoubtedly the largest sources of error. Our ability to quantitatively predict overall kinetics is limited now primarily by the accuracy with which the individual rate parameters are known or can be estimated, rather than other computational modeling issues. The advent of general-purpose reaction-scheme-generation programs places a renewed emphasis on the importance of developing accurate rate-estimation techniques and provides an efficient way to use those rate-estimation rules that are already available. It is hoped that improved empirical and theoretical estimates for $k(T,P)$ will soon be developed for additional reaction systems, allowing construction of more accurate chemical kinetic models for a broader range of application.

Acknowledgment

J.M.G. acknowledges the generous time and discussions spent with Prof. Joseph Bozzelli regarding the details of chemically activated reaction systems. All of the detailed group additivity values used in the automated thermochemical estimation procedures have been developed through his research group at the New Jersey Institute of Technology. All authors acknowledge the computer programming assistance of Dr. Pawel Peczak of ExxonMobil Research and Engineering and Mr. David M. Matheu of MIT. W.H.G. acknowledges financial support from the Division of Chemical Sciences, Office of Basic Energy Sciences, Office of Energy Research, U.S. Department of Energy, under Grant DE-FG02-98ER14914.

Literature Cited

(1) Chevalier, C.; Pitz, W. J.; Warnatz, J.; Westbrook, C. K.; Melenk, H. Hydrocarbon Ignition: Automatic Generation of Reaction Mechanisms and Applications to Modeling of Engine Shock. *Proc. Combust. Inst.* **1992**, *24*, 1362−1367.

(2) Chinnick, S. J.; Baulch, D. L.; Ayscough, P. B. An Expert System for Hydrocarbon Pyrolysis Reactions. *Chemom. Intell. Lab. Syst.* **1988**, *5*, 39−52.

(3) DiMaio, F. P.; Lignola, P. G. KING, a Kinetic Network Generator. *Chem. Eng. Sci.* **1992**, *51*, 2713−2718.

(4) Dente, M.; Pierucci, S.; Ranzi, S. E.; Bussani, G. New Improvements in Modeling Kinetic Schemes for Hydrocarbon Pyrolysis Reactors. *Chem. Eng. Sci.* **1992**, *47*, 2629−2634.

(5) Blurock, E. S. Reaction: System for Modeling Chemical Reaction. *J. Chem. Inf. Comput. Sci.* **1995**, *35*, 607−616.

(6) Prickett, S. E.; Mavrovouniotis, M. L. Construction of Complex Reaction Systems III. An Example: Alkylation of Olefins. *Comput. Chem. Eng.* **1997**, *21*, 1325−1337.

(7) Tomlin, A. S.; Turányi, T.; Pilling, M. J. Mathematical Tools for the Construction, Investigation and Reduction of Combustion Mechanisms. In *Low-Temperature Combustion and Autoignition*; Pilling, M. J., Ed.; Comprehensive Chemical Kinetics Series; Elsevier: Amsterdam, 1997; Vol. 35, Chapter 4.

(8) Glaude P. A.; Warth, V.; Fournet, R.; Battin-Leclerc, F.; Scacchi, G.; Come, G. M. Modelling of the Oxidation of *n*-Octane and *n*-Decane Using Automatic Generation of Mechanisms. *Int. J. Chem. Kinet.* **1998**, *30*, 949−959.

(9) Broadbelt, L. J.; Stark, S. M.; Klein, M. T. Computer Generated Pyrolysis Modeling: On-the-Fly Generation of Species, Reactions, and Rates. *Ind. Eng. Chem. Res.* **1994**, *33*, 790−799.

(10) Broadbelt, L. J.; Stark, S. M.; Klein, M. T. Termination of Computer-Generated Reaction Mechanisms: Species Rank-Based Convergence Criterion. *Ind. Eng. Chem. Res.* **1995**, *34*, 2566−2573.

(11) Quann, R. J.; Jaffe, S. B. Building Useful Models of Complex Reaction Systems in Petroleum Refining. *Chem. Eng. Sci.* **1996**, *51* (10), 1615.

(12) Susnow, R. G.; Dean, A. M.; Green, W. H., Jr.; Peczak, P.; Broadbelt, L. J. Rate-Based Construction of Kinetic Models for Complex Systems. *J. Phys. Chem. A* **1997**, *101* (20), 3731−3740.

(13) Dean, A. M. Detailed Kinetic Modeling of Autocatalysis in Methane Pyrolysis. *J. Phys. Chem.* **1990**, *94*, 1432−1439.

(14) Kiefer, J. H.; Tranter, R. S.; Wang, H.; Wagner, A. F. Thermodynamic Functions for the Cyclopentadienyl Radical: The Effect of Jahn−Teller Distortion. *Int. J. Chem. Kinet.* **2001**, *33*, 834−845.

(15) Matheu, D. M.; Aghalayam, P.; Green, W. H., Jr.; Grenda, J. M. Capturing Pressure-Dependence in Automated Mechanism Generation for Pyrolysis and Combustion. In *Book of Abstracts: 17th International Symposium on Gas Kinetics*; IPTC, Universität Essen: Essen, Germany, 2002.

(16) Ugi, I.; Bauer, J.; Brandt, J.; Freidrich, J.; Gasteiger, J.; Jochum, C.; Schubert, W. New Applications of Computers in Chemistry. *Angew. Chem., Int. Ed. Engl.* **1979**, *18*, 111−123.

(17) Tarjan, R. E. Graph Algorithms in Chemical Computation. In *Algorithms for Chemical Computations*; Christofferson, R. E., Ed.; American Chemical Society: Washington, DC, 1977.

(18) Grenda, J. M.; Dean, A. M.; Green, W. H., Jr.; Peczak, P. K. Recent Advances in Automated Kinetic Mechanism Generation. Presented at the Work-in-Progress Poster (WIPP) Session, at the 27th International Symposium on Combustion, Boulder, CO, Aug 2−7, 1998.

(19) Grenda, J. M.; Bozzelli, J. W.; Dean, A. M. Automated Methods of Treating Chemically Activated Reactions in Kinetic Mechanism Generation. In *Book of Abstracts: Eighth International Conference on Numerical Combustion*; Presented at the Eight SIAM International Conference on Numerical Combustion. Amelia Island, FL.

(20) Grenda, J. M.; Bozzelli, J. W.; Dean, A. M. Automated Group Additivity Estimation of Thermodynamics for Use in Computational Mechanism Generation. Presented at the Work-in-Progress Poster (WIPP) Session, at the 27th International Symposium on Combustion, Boulder, CO, Aug 2−7, 1998.

(21) Grenda, J. M.; Androulakis, I. P.; Bozzelli, J. W. Combined Use of Automated Kinetic Mechanism Generation and Reduction in the Development of Chemical Reaction Models. In *Proceedings of 2nd Joint Meeting of the U.S. Sections of the Combustion Institute*; The Combustion Institute: Pittsburgh, PA, 2001.

(22) Matheu, D. M.; Lada, T. A.; Green, W. H., Jr.; Dean, A. M.; Grenda, J. M. Rate-Based Screening of Pressure-Dependent Reaction Networks. *Comput. Phys. Commun.* **2001**, *138*, 237−249.

(23) Matheu, D. M.; Green, W. H., Jr.; Grenda, J. M. Computational Application of Automated Pressure-Dependent Mechanism Generation: Reaction through Cycloalkyl Intermediates. *Int. J. Chem. Kinet.*, **2003**, *35* (3), 95−119.

(24) Lay, T. H.; Bozzelli, J. W.; Dean, A. M.; Ritter, E. R. *J. Phys. Chem.* **1995**, *99*, 145−85.

(25) Bozzelli, J. W.; Chang, A. Y.; Dean, A. M. *Combust. Sci. Technol.* **1991**, *80*, 63−85.

(26) Green, W. H.; Barton, P. I.; Bhattacharjee, B.; Matheu, D. M.; Schwer, D. A.; Song, J.; Sumathi, R.; Carstensen, H. H.; Dean, A. M.; Grenda, J. M. Computer Construction of Detailed Chemical Kinetic Models for Gas-Phase Reactors. *Ind. Eng. Chem. Res.* **2001**, *40*, 5362−5370.

(27) Sumathi, R.; Green, W. H. A priori Rate Constants for Kinetic Modeling. *Theor. Chem. Acc.* **2002**, *108*, 187−213.

(28) Sumathi, R.; Carstensen, H. H.; Green, W. H. Reaction Rate Prediction via Group Additivity, Part 2: H Abstraction from Alkenes, Alkynes, Alcohols, and Acids by H Atoms. *J. Phys. Chem. A* **2001**, *105*, 8969−8984.

(29) Curran, H. J.; Gaffuri, P.; Pitz, W. J.; Westbrook, C. K. A comprehensive modeling study of *n*-heptane oxidation. *Combust. Flame* **1998**, *114* (1−2), 149−177.

(30) Truong, T. N. Reaction Class Transition State Theory: Hydrogen Abstraction Reactions by Hydrogen Atoms as Test Cases. *J. Chem. Phys.* **2000**, *113* (12), 4957−4964.

(31) Ranzi, E.; Dente, M.; Faravelli, T.; Pennati, G. Prediction of Kinetic-Parameters for Hydrogen Abstraction Reactions. *Combust. Sci. Technol.* **1994**, *95* (1−6), 1−50.

(32) Forst, W. *Theory of Unimolecular Reactions*; Academic Press: New York, 1973.

(33) Back, M. H.; Back, R. A. In *Pyrolysis: Theory and Industrial Practice*; Albright, L. F., Crynes B. L., Corcoran, W. H., Eds.; Academic Press: New York, 1983; pp 1−24.

(34) Chen, C. J.; Back, M. H.; Back, R. A. *Can. J. Chem.* **1976**, *54*, 3175−3184.

Received for review July 30, 2002
Revised manuscript received December 16, 2002
Accepted December 16, 2002

IE020581W